Research on factors influencing stability of Subgrade Soil Cave in karst area based on Soil Arching Effect

Di Wu, Haoran Wang, Taiming Liang, Wenwu Chen *

Guilin University of Electronic Technology, Guilin, Guangxi, China

*Corresponding author: 340070812@qq.com

Abstract. In karst areas of China, subgrade cave collapse is a serious threat to traffic safety. In this paper, numerical simulation and experimental validation are used to examine the effects of different collapse widths, fill heights, and cohesive forces on the stability of subgrade soil caves. The results of the experiment indicate that with the increase of collapse width, the load sharing in the stable area increases, and the stability of the soil caves decreases. The stability area's load distribution increases with increasing filling height, however the filling height has no effect on the stability area's overall change trend in terms of soil pressure. The greater the cohesion, the smaller the load sharing in the stable region, indicating that the stability of the soil caves increases with the increase of cohesion.

Keywords: Subgrade; Karst area; Soil arching effect; Soil cave stability; Influencing factors.

1 Introduction

According to statistics, there are 42,420 kilometers of existing roads in China's karst regions, 7,349 kilometers of existing roads in locations with an extremely high risk of collapse, and 5735 kilometers of existing roads in areas with a high risk of subgrade soil cave collapse [1]. There is a wide range of subgrade soil caves in the karst area, thus the affected area is also large. Due to their underground location and difficulty in detection, these subgrade soil caves can quickly result in serious safety issues such pavement collapse and subgrade subsidence [2].

In nature, subgrade soil caves can maintain self-stability to a certain extent due to the interaction of factors such as geotechnical physical properties around soil caves, groundwater flow characteristics, and surface current erosion [3]. Through an in-depth study of the action mechanism and influencing factors of soil cave self-stability, we can better understand the formation and evolution process of subgrade soil caves, and provide a scientific basis and effective measures for subgrade soil cave engineering construction [4]. In addition, this research can also offer a crucial reference for disaster prevention and ecological environmental protection of subgrade and pavement in karst areas in order to ensure people's safety and sustainable development [5].

P. Xiang et al. (eds.), *Proceedings of the 2023 5th International Conference on Hydraulic, Civil and Construction Engineering (HCCE 2023)*, Atlantis Highlights in Engineering 26,
https://doi.org/10.2991/978-94-6463-398-6_54

The stability of soil caves has always been a significant study area in the realm of soil mechanics and geoengineering. At the end of the 20th century and the beginning of the 21st century, the research on soil arching effect has been more extensive, and the corresponding theoretical and experimental research has been deepened and expanded. George and Dasaka [6] conducted a numerical simulation of a kind of trapdoor mechanism, proposed the stress transfer balance problem in soil arching, emphasized the significant characteristics of equivalent settling plane and critical height, and revealed the necessity of further understanding of arch in various field applications. To explore the micromechanical mechanism of soil arching, Ali Umair and Otsubo Masahide et al. [7] used two particle shapes (spherical particles and non-spherical particles) to conduct complementary discrete element simulation. Einar Broch et al. [8] studied the reinforcement effect of full grouting bolts and tension bolts on the roof and wall of the cavern and the influence on the arch formation of the roof of the cavern by numerical simulation and application of arch theory. Jaeyeon Cho et al. [9] studied the vertical circular shaft by combining experimental and numerical analysis, found that when the arch effect is considered, the lateral soil pressure of the vertical circular shaft is about 80% lower than that calculated by Rankine theory. The soil arching effect disperses the external load to the soil around the soil cave, thus reducing the bearing pressure of the soil cave and increasing its stability.

A numerical analysis model corresponding to the scale model was established using the PLAXIS3D numerical simulation software in order to study the load sharing in the stable area/subsidence area and to verify it with the results of the soil pressure test of the scale model to ascertain the accuracy of the stability of the soil cave under the soil arching effect. Meanwhile, three variables of different collapse widths, fill heights, and cohesion were set to study the impact on the load sharing in the stable zone and collapse zone of the subgrade.

2 Numerical simulation

2.1 The establishment of computational model

The 3D numerical simulation model consists of three parts: virtual baffle, filling with different properties, and collapse area with vertical displacement. Base on numerical simulation, a numerical simulation model was established and verified by existing model tests such as Wu [10]. Considering the boundary effect generated by numerical simulation, the model size was set as 30m×30m×5m (length × width × height), and the collapse surface was a circular. Based on the symmetry of the model test device, the model shown in Figure 1 was established. In this model, 15-node triangular units and subgrade soil as drainage was selected, and the boundary conditions were horizontal constraints. The subsidence depth of the subsidence area was determined by specifying displacement, and the groundwater level was set to the position of -1000m above sea level, where the altitude did not influence on the test, and the monitoring points were selected in the gray box in Figure 1, as shown in Figure 2. The information about monitoring points is described in Table 2. The selection of simulation parameters was showed in Table 1, which mainly based on the soil test data and some experience.

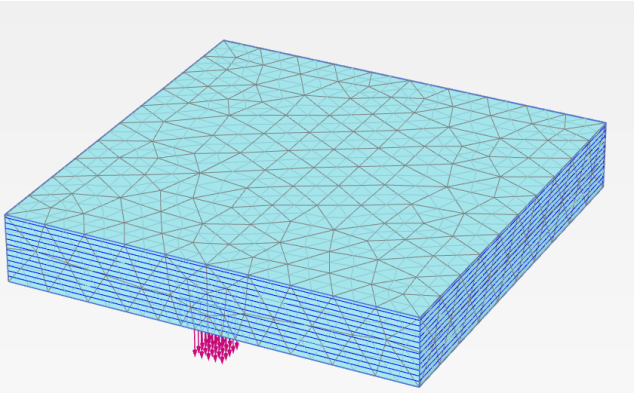

Fig. 1. numerical calculation model

Table 1. Numerical simulation of subgrade working arrangement

Research contents	Simulated subgrade condition	Cohesion c/kPa	Depth of fill H/m	Collapse radius R/m
Collapse width effect	Z1	1	5	0.75
	Z2	1	5	0.5
	Z3	1	5	0.25
Fill height influence	Z4	1	3	0.75
	Z5	1	1	0.75
The effect of cohesion	Z6	10	5	0.75
	Z7	20	5	0.75

Table 2. Some information from the model

Points at the bottom horizontal position of the model	**Y1**	**Y2**	**Y3**	**Y4**	**Y5**	**Y6**	**Y7**	**Y8**	**Y9**	**Y10**
Distance from collapse center Y0/m	0.2	0.6	0.8	1.1	1.6	1.9	2.4	3.3	4.3	7.3
Vertical point selection for collapse	H1		H2		H3		H4	H5	H6	H7
Distance from collapse center Y0/m	0.2		0.5		0.7		0.8	0.9	2.4	3

2.2 Verification of computational models

To verify the feasibility of numerical simulation, a standard group with the same soil parameters as the numerical simulation was set up for the scaled model test. Figure 2 shows the comparison between the numerical simulation standard group and the scaled model test results. It can be seen that the numerical simulation is similar to the scaled model test results. From the periphery of the roadbed collapse zone to the inside of the

stable zone, the soil pressure shows a tendency of increasing and then dropping, while the soil pressure in the subsidence area decreasing and finally approaches 0. The stable zone of the subgrade is responsible for bearing the over soil pressure under the impact of the soil arching effect. It is confirmed that the scale model tests and numerical simulations employed in examining the stability mechanism of soil cavities under the action of soil arching are correct.

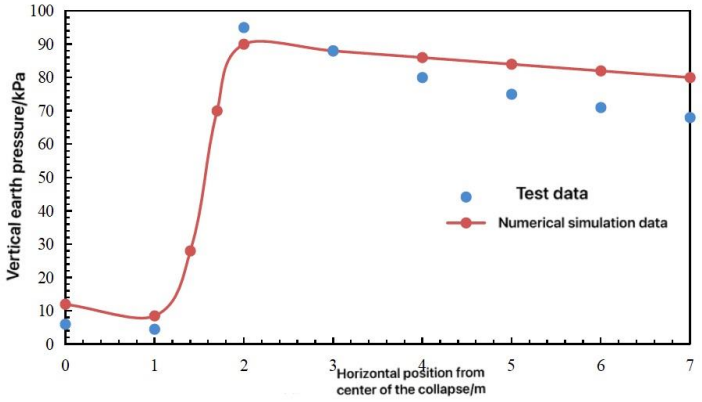

Fig. 2. Comparison of soil pressure test values with numerical simulation

3 Load sharing in subgrade stabilization area/subsidence area based on soil archING effect

3.1 The influence of collapse width

In order to study the influence of different collapse widths of the stability of soil caves, groups Z2 and Z3 were set respectively to compare the subgrade working conditions, and the vertical collapse displacement is 0.3m.

Figure 3 (a) shows the results of soil pressure at point Y1, the soil pressure under three different subgrade conditions shows a rapid decrease before the collapse of 0.01m. As the collapse continues, the soil pressure under three different subgrade conditions with different collapse widths is 24.247kN, 12.813kN, and 30.691kN, respectively. However, under the Z2 and Z3 subgrade conditions, the soil pressure hovered around 0.4kN and 1.5kN respectively after a collapse of 0.01m, while the soil pressure of Z1 changed from 28.5kN to 26.4kN from a collapse of 0.01m to a collapse of 0.3m, which shows a decreasing trend compared to point Y1.

Figure 3 (b) shows the results of soil pressure at point Y6. The subgrade with a 3 m collapse width has a quick increase in soil pressure as a result of the soil arching effect. When the soil collapses by 0.01m, the soil pressure reaches 103.9kN and 96.947kN respectively. At both points, the other two subgrade conditions show a quick increase at first, followed by a moderate increase.

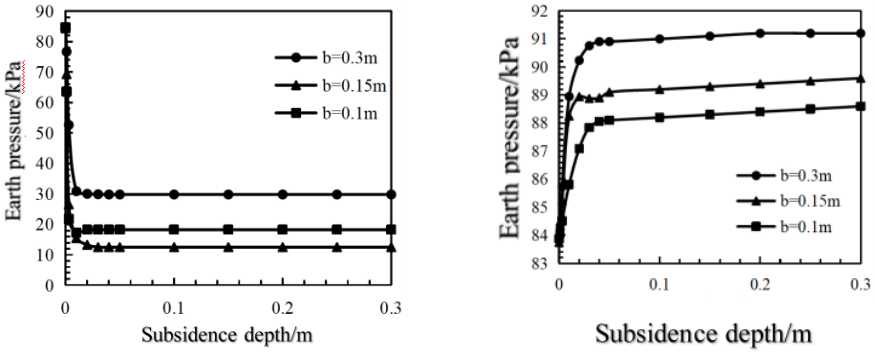

(a)Y1 (b)Y6

Fig. 3. Soil pressure distribution curve

3.2 Effect of filling height

To study the influence of different filling heights on the stability of soil caves, two groups Z4 and Z5 were set to compare the subgrade working conditions, and the vertical collapse displacement is also set 0.3m.

Figure 4 (a) shows the results of soil pressure at point Y1. The soil pressure of three types of collapse widths rapidly decreases when the settlement is about 0.01m. Among them, the soil pressure of the subgrade conditions with filling heights of 1m and 3m tends to zero as the settlement continues after 0.01m, while the soil pressure of the subgrade conditions with filling heights of 5m fluctuates around 12kN as the settlement continues after 0.01m. Figure 4 (b) shows the results of soil pressure at point Y4, all three subgrade conditions show an increasing trend before the collapse of approximately 0.01m. As the collapse continue, the soil pressure at point Y4 shows a decreasing trend. After the settlement of 0.3m, the soil pressure under the three subgrade conditions is 14.985kN, 54.28kN, and 79.087kN, respectively.

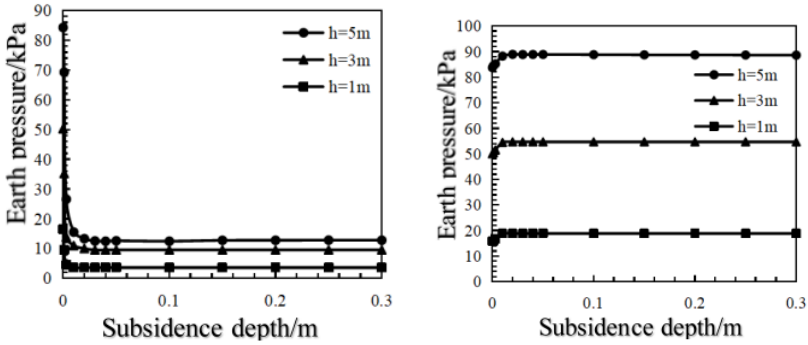

(a) Y1 (b)Y4

Fig. 4. Soil pressure distribution curve

The numerical simulation demonstrates that there is no clear variation trend in soil pressure for various filling heights. In group Z1, Z4 and Z5, the variation trend of soil pressure is consistent with the soil pressure in the test data.

3.3 The effect of cohesion

In the case that the numerical simulation of different collapse widths and fill heights is consistent with the test data, the soil pressure changes in the subgrade working conditions Z6 and Z7 are compared by adding different cohesion forces, and the vertical collapse displacement is 0.3m.

Figure 5 (a) shows the results of soil pressure at point Y1. After a settlement of 0.3m, the soil pressure at point Y1 with different cohesive forces decreases from 84.34kN to 12.81kN, 0.35kN, and 0.014kN, respectively. During the settlement process, the soil pressure at point Y1 rapidly decreases after a settlement of 0.01m, and then the soil pressure roughly changes in a linear function with a constant of 0. Only the soil pressure of point Y1 reduce to 12.813kN when c is 1 kPa. In other cases, the soil pressure in the collapsed area decrease to nearly 0kN, and the simulation results shows that the higher the cohesion, the smaller the soil pressure during the subsidence process.

Take Y4 and Y6 in the stable zone of the subgrade as an example, with the two points separating from Y0 point 1.6m and 2.4m. In Figures 5 (b) and Figures 5 (c), with a cohesive force of 1kPa, the soil pressure at both points shows an increasing trend before the collapse of 0.01m. The soil pressure increases to 91.35kN and 88.94kN respectively due to the soil arching effect, but decrease exponentially as the collapse progressed. After the settlement of 0.3m, the soil pressure decreases to 79.09kN and 88.63kN respectively. As the distance from Y0 point increase, the soil arching effect become less significant, and the value of soil pressure begin to increase; When c is 10kPa, the soil pressure increases sharply before the settlement of 0.01m in the collapsed area. When it continues to settle to 0.3m, the soil pressure is 90.7kN and 85.86kN, respectively. The reason for the decrease in soil pressure is the same as when c is 1kPa, and will not be repeated here.

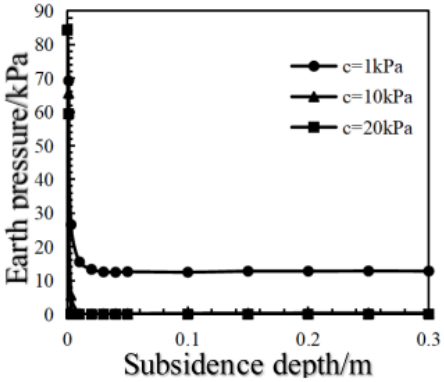

(a)Y1

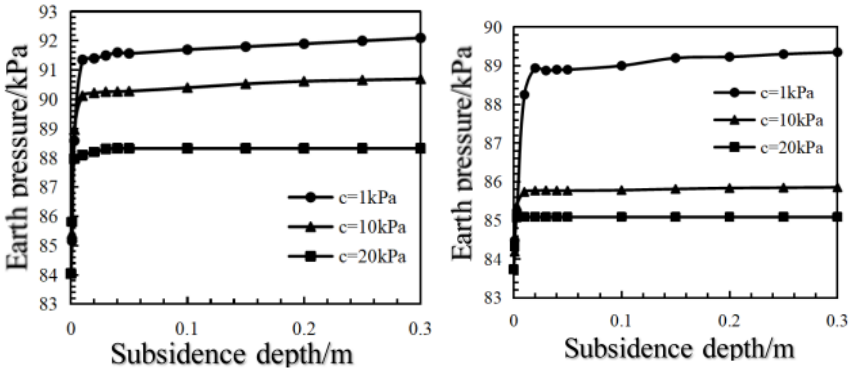

(b)Y4 (c)Y6

Fig. 5. Soil pressure distribution curve

When c is 20kPa, the same soil pressure increases to the maximum at about 0.01m of subsidence, and then decreases exponentially with subsidence. The soil pressure at the four points is 66.19kN, 82.10kN, 83.21kN and 83.05kN, respectively. It can be seen from the Y6 point soil pressure diagram that the greater the cohesion, the shorter the distance of soil arching effect.

According to the trend that the greater the cohesion, the greater the soil pressure in the stable area of the subgrade, it can be seen that the greater the cohesion, the smaller the soil arching generated during the collapse process, and the smaller the vertical influence height. Under the effect of the soil arching, the soil pressure transferred from Shear stress to the stable area under the soil arching effect is relatively small, and the stability of the soil cave is higher.

4 Discussion

In this testing, PLAXIS3D was used to study the stability mechanism of soil cavity, and the standard set of numerical simulation scaling model test and corresponding parameters were set. The load sharing between subsidence area and stable area was analyzed through numerical simulation, indicating that the load transfer of overburden soil layer to stable area under the action of soil arch effect ensured the stability of soil cavity. At the same time, three comparison conditions of different collapse widths, filling heights and cohesiveness are established to verify whether different factors affect the stability of soil caves. Based on previous researchers, the influence of soil arch effect on subgrade soil caves is further studied.

5 Conclusion

In this paper, PLAXIS3D is used to study the stability mechanism of soil caves and draw the following conclusions:

The soil caves transfer the load from the subsidence area to the stable area through the soil arching effect, which makes the soil cave stable. Through numerical simulation of subgrade with different collapse widths, fill heights and cohesive forces, it is concluded that: the stability of soil cave is closely related to the collapse width. With the increase of the collapse width, the load sharing in the stable region increases and the stability of the soil tunnel becomes weak, which is consistent with the results of the scale model test. It can be seen that the higher the filling height, the greater the load sharing in the stable area. The filling height has no effect on the stability area's overall change trend in terms of soil pressure, which indicating that the filling height has little effect on the stability of the soil cave, which is consistent with the results of the scale model test. Finally, it is found that the greater the cohesion, the smaller the load sharing in the stable region, indicating that the stability of soil cavity becomes stronger as the cohesion increases.

Funding

This research was supported by the National Natural Science Foundation of China Grant (No. 42067044) and the Key Science and Technology Project of Guangxi Grant (AB23026028).

References

1. Lee, J. H., Jung, D. H., & Kim, D. K. (2018). Study on soil arching effect in geosynthetic reinforced earth retaining walls by centrifuge modeling. Geosynthetics International, 25(5), 462-474.
2. Park, H. K., & Kim, D. H. (2015). Experimental study on soil arching effect in geogrid-reinforced retaining walls. Geotextiles and Geomembranes, 43, 127-135. DOI: 10.1016/j.geotexmem.2014.11.001.
3. Sairam, M. V., & Sitharam, T. G. (2018). Soil arching in geocell-reinforced retaining walls: a numerical study. Geotextiles and Geomembranes, 46, 189-198.
4. Singh, A. K., & Singh, R. (2019). Experimental investigation on soil arching effect in geosynthetic-reinforced soil retaining walls. Geotextiles and Geomembranes, 47, 617-627. DOI: 10.1016/j.geotexmem.2019.04.004.
5. Schuppener, B., Krumpholz, S., & Pimentel, E. (2019). Soil-arch action in geogrid-reinforced slopes with crest loads: numerical investigation. Geotextiles and Geomembranes, 47(6), 812-823. doi: 10.1016/j.geotexmem.2019.07.002.
6. George Tharakan Idiculla, Dasaka Satyanarayana Murty. Numerical Investigation of Soil Arching in Dense Sand[J]. International Journal of Geomechanics, 2021, 21(5).
7. Ali Umair, Otsubo Masahide, Ebizuka Hiroaki, Kuwano Reiko. Particle-scale insight into soil arching under trapdoor condition[J]. Soils and Foundations2020, 60(5).
8. Huang Ziping,Einar Broch, Lv Ming. Formation and anchorage of roof arch of underground powerhouse of hydropower station [J]. Chinese Journal of Rock Mechanics and Engineering,2005(08):1348-1354.Cho, J., Choi, H., Kim, K., & Lee, J. (2018). Experimental and Numerical Study on Soil Arching Effect for a Geosynthetic Reinforced Soil Wall. KSCE Journal of Civil Engineering, 22(1), 185-191.

9. Singh, Y. (2018). Analysis of Soil Arching in Reinforced Soil Walls using Finite Element Method. International Journal of Civil Engineering and Technology, 9(10), 1778-1787.
10. Wu, D., Luo, C., Li, YK., Yang, YX., Liang, YH., &Wu,JJ (2021). Application of a Geotextile in the Treatment of Post-Subsidence in Karst Areas. Applied Sciences, 11(24), 11826.